ChemComm

Accepted Manuscript

ROYAL SOCIETY OF CHEMISTRY

rsc.li/chemcomm

View Article Online
DOI: 10.1039/C7CC04599A

Journal Name

COMMUNICATION

Structural stability of the photo-responsive DNA duplexes containing one azobenzene via a confined pore

Received 00th January 20xx,
Accepted 00th January 20xx

DOI: 10.1039/x0xx00000x

www.rsc.org/

Fu-Na Meng,‡ Zi-Yuan Li,‡ Yi-Lun Ying,* Shao-Chuang Liu, Junji Zhang and Yi-Tao Long

Here, the structural stability of single azobenzene modified DNA duplexes, including the *trans* form and *cis* form, has been examined separately based on their distinguishable unzipping kinetics from the mixture by an α-hemolysin nanopore. Further, the accurate isomerization efficiency between the *trans* and *cis* form was obtained with single molecule resolution.

Photo-responsive DNA modified with azobenzene is an attractive design for efficiently photo-regulating DNA functions and DNA nanomachines.[1,2] For example, based on the azobenzene-modified photo-responsive DNA, DNA replication, transcription and other enzyme activity achieved to be regulated by artificial operation.[3–5] Similarly, DNA nanomachines, extraordinarily promising in molecular sensing, logic gate operating and drug delivering, also could be controlled by light utilizing the photo-responsive DNA, which avoided the addition of molecular fuels for each working cycle.[6–8] The essential of the photo-controlling DNA is to regulate the azobenzene-modified DNA duplex (azo-dsDNA) stability imparted by photo-responsive azobenzene for ultimate hybridization/dissociation.[9] However, the structural stability of photo-responsive DNA duplex imparted by single azobenzene was rarely reported. The main reason is that there exist lots of difficulties in discriminating the *trans* form and *cis* form of azo-dsDNA from the mixtures. For example, although melting curves[9] may provide the structural stability of the *trans* form and *cis* form of azo-dsDNA combining with calculations, such measurement would be difficult owing to two reasons. First, an expected Tm change by one azobenzene could be very small. Second, even if the small variation could be monitored, the results were derived from the ensemble solution not reflected the *trans* form and *cis* form, respectively. Therefore, probing the structural stability by different way is necessary.

The α-hemolysin (α-HL) nanopore,[10] a single molecule tool, has been proven as an ultra-sensitive system for the determination of individual molecules, such as ssDNA,[11,12] peptides,[13,14] proteins[15,16] and host-guest molecules.[17,18] Previous researches have incorporated α-HL nanopores for studying the duplex structural stability influenced by a single base lesion.[19,20] In this paper, we employed electrochemical confined effect of α-HL nanopore to discriminate the *trans* form and *cis* form of azo-dsDNA from the mixtures and explore their structural stability, respectively (Fig. 1). The azo-dsDNA was electrochemically driven into the nanopore following by sequentially unzipping and translocating through the pore. The confined space in α-HL converts the structural stability of

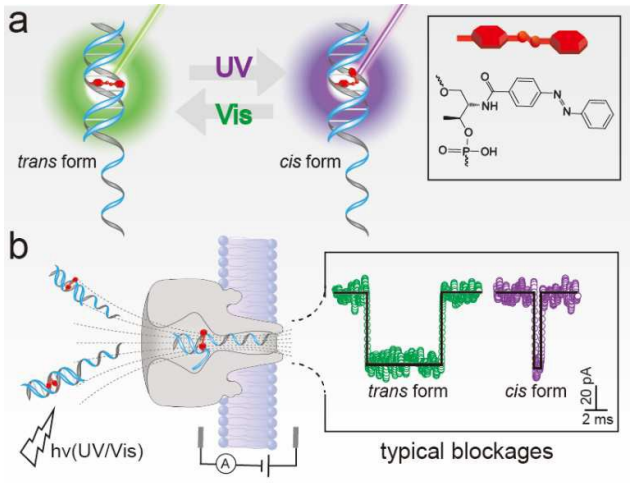

Fig. 1 (a) Schematic illustration of the reversible conversion between the *trans* and *cis* form of azo-dsDNA by photo regulation. A single azobenze moiety is shown in red color. (b) Discrimination of the *trans* and *cis* form of azo-dsDNA from the mixture by an α-HL nanopore. The α-HL nanopore inserted into a lipid bilayer. The two chambers beside the nanopore were termed as cap side and stem side, respectively. Individual azo-dsDNA in the cap side chamber unzips and traverses the α-HL nanopore. The *trans* form of azo-dsDNA generated the blockages with longer unzipping time than the *cis* form, which showed the high structural stability of the *trans* form. The voltage was applied using a pair of Ag/AgCl electrodes. The illustration was not to scale.

Key Laboratory for Advanced Materials & School of Chemistry and Molecular Engineering, East China University of Science and Technology, Shanghai 200237, P. R. China.
Email: yilungying@ecust.edu.cn; Fax: +86-21-64250032; Tel: +86-21-64250032
‡ These authors contributed equally to this work.
†Electronic Supplementary Information (ESI) available. DOI: 10.1039/x0xx00000x.

View Article Online
DOI: 10.1039/C7CC04599A

individual azo-dsDNA into distinguishable kinetic unzipping information. Compared to the native duplex, the *trans* form are about 7 times more stable and the *cis* form around 2 times less stable. Further, our method achieves to provide an isomerization efficiency of around 46% (*trans*-to-*cis*) and 71% (*cis*-to-*trans*) for the photo-regulated azo-dsDNA based on single molecule discrimination. The accurate isomerization efficiency is a vitally important parameter for evaluating the photo-controlled DNA nanostructures.

The random sequence of azo-ssDNA and its complementary DNA (c-ssDNA) was as follows:

azo-ssDNA 5'-CGATC-X-CTAGC-3'

c-ssDNA 5'-GCTAG----GATCG-$(C)_{30}$-3'

One azobenzene group was introduced into position X through a D-threoninol group (Fig. S1-S14). The azo-dsDNA was formed with the azobenzene group intercalating between adjacent base pairs as demonstrated in previous researches[2,21]. The double-stranded segment was followed by a poly$(dC)_{30}$ overhang via annealing (see ESI†). The overhang will help the DNA duplex to be captured by α-HL nanopore easily and then the unzipping events of the duplex can be obtained in quantity.

First, to obtain more *cis* form of the azo-dsDNA, the annealed solution was irradiated with UV light for 5 min at 58 °C. Then, the solution was added into the cap side chamber at dark. It produced lots of blockage events at +80 mV. We extracted the duration times and I/I_0 of the events for statistic. Here I was defined as the blockage residue current and I_0 as the open pore current. In the 2D contour plots, there was one population distributed in the region with duration less than 0.20 ms (Fig. 2a), which may come from the unbind ssDNA (Fig. S15, ESI†). Additionally, the collision behavior of the dsDNA with the nanopore also might induce these short-lived events. Noticed that there is another clear distribution with long duration (over 0.2 ms) and deep current amplitude with I/I_0 less than 0.23. Since the ssDNA in the solution only induced short-lived events (Fig. S15, ESI†), the population with duration over 0.2 ms was ascribed to the azo-dsDNA. According to the previous research,[20] this population was derived from the duplexes unzipping through the α-HL nanopore (Fig. 1b). Typically, the unzipping duration of a double-stranded DNA within the α-HL nanopore is much longer than the translocation time of the ssDNA at the same applied potentials.[19,22] Therefore, the duration of these current blockages is deemed as the unzipping times for extracting kinetic information of strand dissociation related to the duplex stability. The duration of the azo-dsDNA was fitted into a double exponential function and two distribution peaks, P1 and P2, were obtained (Fig. 2b). This demonstrate that there existed two unzipping time constants for azo-dsDNA, which might be corresponding to the *trans* and *cis* form, respectively. Accordingly, the population in 2D plots was divided into population P1 and P2 for the following clear statement (Fig. 2a).

To further determine the assignment of these two populations, visible light, which could convert the *cis* to *trans* form of azo-dsDNA, was used to irradiate the solution in the

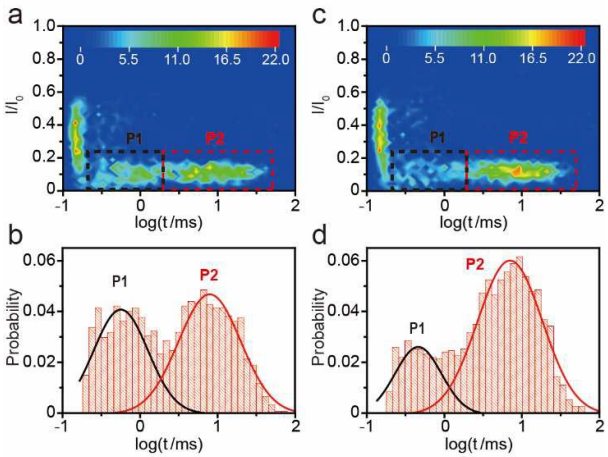

Fig. 2 The 2D contour plots (upper) and the duration (t) histograms (bottom) of the unzipping evens for the annealed DNA solution containing azo-dsDNA after irradiation by UV (a, b) and *vis* light (c, d), respectively. Both the 2D plots were composed of 2500 blockage events. The duration distributions were fitted by a double exponential function and the fitted parameters were shown in Table S1. Both the histograms were composed of 1550 events. The experiments were conducted in solutions containing 1.0 M KCl buffered with 10 mM Tris and 1 mM EDTA (pH = 8.0) at +80 mV.

cap side chamber for 10 min. As shown in Fig. 2c-d, the solution also induced P1 and P2 in both the 2D plot and the duration histogram for the unzipping events. Compared to the results under UV irradiation, the event count of P1 decreased and that of P2 increased evidently in the 2D plot and the histogram (Fig. 2). These results demonstrated that UV caused P1 increasing and *vis* induced P2 rising. To further confirm this phenomenon, the frequencies for population P1 and P2 were also analyzed after UV and *vis* irradiation, respectively (Fig. 3a). The frequencies of population P1 and P2 under UV irradiation were 6.0 ± 1.2 and 6.5 ± 0.9 min^{-1}, respectively (Table S2). When switched to *vis* light, the frequency of P1 decreased to 2.8 ± 0.5 min^{-1}, while P2 increased to 9.6 ± 1.6 min^{-1}. This further shows UV light induces P1 increasing and *vis* gives rise to P2. It is convinced that UV light could convert the azo-dsDNA from *trans* to *cis* form and on the other hand, *vis* could contribute to the *trans* form.[1] Thus, P1 was ascribed to the *cis* form and P2 was assigned to the *trans* form of the azo-dsDNA. The fitted values of P1 and P2 in the duration histogram were regarded as unzipping time constants (τ) for the separate *cis* and *trans* form through the α-HL nanopore, which are 0.52 ± 0.01 and 8.07 ± 0.36 ms at +80 mV, respectively. As well as the duration histograms of the two isomers were both well described by single exponential function, the rate constants (k) of the unzipping process were acquired using the following equation[23]:

$$k=1/\tau$$

Thus, the rate constants of duplex dissociation for *cis* form and *trans* form were, respectively, 1920 ± 400 s^{-1} and 124 ± 15 s^{-1} at +80 mV. The structural stability of the duplexes is interpreted in terms of their kinetic results.[19] Therefore, the duplex conformation containing *trans*-azobenzene is more stable, while the *cis*-azobenzene instead facilitates the strand dissociation relative to the native duplex. The *trans* form with

View Article Online
DOI: 10.1039/C7CC04599A

high stability has to overcome higher energy barrier to unzip through the nanopore and thus needs more time to endure the electrical force.

Moreover, the native DNA duplex was analyzed via an α-HL nanopore to compare with the azo-dsDNA. The native duplex was formed via the hybridization between the native ssDNA (5'-CGATCCTAGC-3') and c-ssDNA. Similarly, lots of unzipping events were induced by the native duplex (Fig. S15 and S16, ESI†). In the duration histogram for the unzipping events, the distribution followed a single exponential function (Fig. 3b), rather than a double exponential distribution of azo-dsDNA. UV and *vis* irradiation hardly affected the histogram distribution (Fig. S17, ESI†), which further demonstrated that the double exponential distribution for azo-dsDNA resulted from the incorporation of azobenzene. The unzipping time constant for the native duplex was 3.48 ± 0.47 ms at +80 mV. Thus, the rate constant was 287 ± 32 s^{-1}, which lay between them for *cis* form (1920 ± 400 s^{-1}) and *trans* form (124 ± 15 s^{-1}) of azo-dsDNA. These results demonstrated that the *cis* form has structural instability and *trans* form high stability relative to the native duplex. It is suggested that the nonplanar azobenzene (*cis* form) may interrupt the base stacking and hydrogen bonding to destabilize the duplex relative to the native duplex. While the planar azobenzene (*trans* form) may enhance the base stacking to stabilize the duplex.

The unzipping events of azo-dsDNA and the native duplex were also studied at different potentials ranging from +70 to +110 mV (Fig. 3c and Fig. S18-S19, Table S1 and S3, ESI†). The unzipping time constant for the *cis* form decreased from 0.58 ± 0.02 to 0.34 ± 0.02 ms and that for the *trans* form reduced from 12.30 ± 0.41 to 2.01 ± 0.23 ms exponentially with the voltage increasing from +70 to +110 mV (Fig. 3c and Table S4, ESI†). The unzipping time constant of the native duplex always lay between the two isomers of azo-dsDNA, exponentially dropping from 7.59 ± 0.35 to 0.78 ± 0.08 ms with the rising potential from +70 to +110 mV. These results not only further confirmed the unzipping translocation of the duplexes through the nanopore[20] but also showed that the duplex stability of the *trans* form and the instability of the *cis* form relative to the native one were independent of the potentials. Noted that the subtle difference of the structural stability was enlarged at low potential. As shown in Fig. 3c, the τ gap (Δτ) be-tween the *cis* form of azo-dsDNA and native duplex decreased from 7.01 to 0.44 ms and that between the *trans* form and the native one reduced from 4.72 to 1.23 ms as the potential grew from +70 to +110 mV. This might originate from that the activation energy of high potential exceeds the unzipping energy barrier and the unzipping behaviour is not limited by the high potential. Although low potential allowed the high sensitivity for detecting the duplex stability, it limited the capture rate of DNA by the nanopore.[24] Thus, +80 mV was chosen for main analysis in our system.

Furthermore, the isomerization efficiency between the *trans* and *cis* form was calculated at single molecule level. Under our experimental conditions, the isomerization efficiency was (46 ± 3) % for *trans*-to-*cis* and (71 ± 7) % for *cis*-to-*trans* (Fig. 3d). These values are comparable to them obtained via the traditional method under the similar experiment conditions, which is about 50% and 85%.[25] The little difference of isomerization efficiency by the two methods not only come from the slight difference of the target duplexes but also originate from the sensitivity of these two methods. The results provided by nanopore technique are much more precise as they are acquired based on single molecule discrimination from the heterogeneous mixture. The accurate isomerization efficiency is an important evaluation index for the reliable and high-efficiency photo-responsive DNA nanodevices.

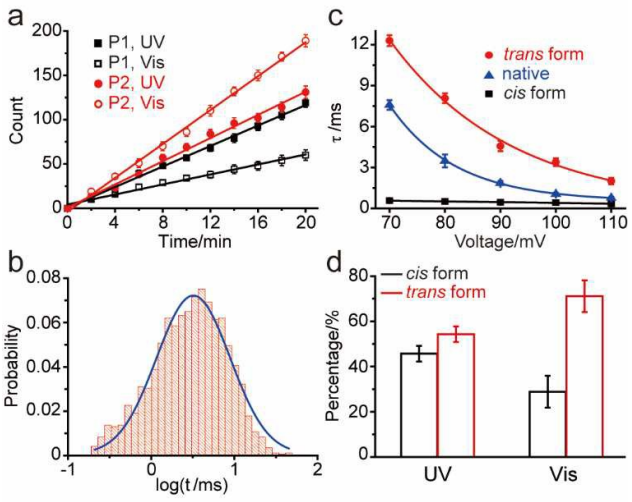

Fig. 3 (a) Cumulative event count versus recording time (min) for population P1 and P2 in the 2D contour plots under UV or *vis* irradiation. The curve was fitted linearly and the fitting parameters were demonstrated in Table S2. (b) Singe exponential distribution of the duration of unzipping events for the native duplex at +80 mV. The fitting parameters were exhibited in Table S3. (c) The unzipping time constant for the native duplex and the *cis* and *trans* form of azo-dsDNA as a function of applied voltage. All the curves were fitted by single exponential function and the fitting parameters were shown in Table S4. (d) The percentages of *cis* and *trans* form of azo-dsDNA under UV and *vis* irradiation, respectively. The percentages were obtained via the corresponding peak area of the duration histogram at +80 mV. The experiments were performed in solutions containing 1.0 M KCl buffered with 10 mM Tris and 1 mM EDTA (pH = 8.0).

In summary, we utilized an α-HL nanopore biosensor to characterize the duplex stability induced by single azobenzene. The kinetic results of duplex dissociation were acquired by the nanopore at single molecule level, which have been interpreted in terms of the structural stability of the duplexes. Our results provide incontrovertible evidence for that single *trans*-azobenzene stabilizes the duplex conformation dramatically, whereas single *cis*-azobenzene facilitates the strand dissociation compared with the native duplex. Further, the isomerization efficiency between the two isomers of the azo-dsDNA was calculated at single molecule level. Besides, the α-HL nanopore biosensor provides a standard for designing an efficient photo-responsive DNA, which is the narrow width of the two unzipping time peaks for the isomers and the large gap between them.

This research was supported by the National Natural Science Foundation of China (21505043, 21421004, 21327807) and the Fundamental Research Funds for the Central Universities

View Article Online
DOI: 10.1039/C7CC04599A

(222201718001, 222201717003, 222201714012). Y. L. Ying is supported by the Chinese Post-doctoral Fund (2016T90340). J. J. Zhang is supported by the National Natural Science Foundation of China (21420102004).

Conflicts of interest

There are no conflicts to declare.

Notes and references

1 Y. Kamiya and H. Asanuma, *Acc. Chem. Res.*, 2014, **47**, 1663–1672.
2 W. Szymański, J. M. Beierle, H. A. V. Kistemaker, W. A. Velema and B. L. Feringa, *Chem. Rev.*, 2013, **113**, 6114–6178.
3 M. Liu, H. Asanuma and M. Komiyama, *J. Am. Chem. Soc.*, 2006, **128**, 1009–1015.
4 A. Yamazawa, X. Liang, H. Asanuma and M. Komiyama, *Angew. Chemie*, 2000, **112**, 2446–2447.
5 M. You, R.-W. Wang, X. Zhang, Y. Chen, K. Wang, L. Peng and W. Tan, *ACS Nano*, 2011, **5**, 10090–10095.
6 Y. Zou, J. Chen, Z. Zhu, L. Lu, Y. Huang, Y. Song, H. Zhang, H. Kang and C. J. Yang, *Chem. Commun.*, 2013, **49**, 8716–8718.
7 Y. Yang, M. Endo, K. Hidaka and H. Sugiyama, *J. Am. Chem. Soc.*, 2012, **134**, 20645–20653.
8 Q. Yuan, Y. Zhang, T. Chen, D. Lu, Z. Zhao, X. Zhang, Z. Li, C.-H. Yan and W. Tan, *ACS Nano*, 2012, **6**, 6337–6344.
9 Y. Nakasone, H. Ooi, Y. Kamiya, H. Asanuma and M. Terazima, *J. Am. Chem. Soc.*, 2016, **138**, 9001–9004.
10 L. Song, M. R. Hobaugh, C. Shustak, S. Cheley, H. Bayley and J. E. Gouaux, *Science*, 1996, **274**, 1859–1865.
11 Y. L. Ying, J. Zhang, R. Gao and Y. T. Long, *Angew. Chemie - Int. Ed.*, 2013, **52**, 13154–13161.
12 Y. Zhang, G. Wu, W. Si, J. Sha, L. Liu and Y. Chen, *Chinese Sci. Bull.*, 2014, **59**, 4908–4917.
13 H. Y. Wang, Z. Gu, C. Cao, J. Wang and Y. T. Long, *Anal. Chem.*, 2013, **85**, 8254–8261.
14 A. Asandei, M. Chinappi, H.-K. Kang, C. H. Seo, L. Mereuta, Y. Park and T. Luchian, *ACS Appl. Mater. Interfaces*, 2015, **7**, 16706–16714.
15 T. Li, L. Liu, Y. Li, J. Xie and H. C. Wu, *Angew. Chemie - Int. Ed.*, 2015, **54**, 7568–7571.
16 X. Hou, W. Guo and L. Jiang, *Chem. Soc. Rev.*, 2011, **40**, 2385–2401.
17 Y.-L. Ying, J. Zhang, F.-N. Meng, C. Cao, X. Yao, I. Willner, H. Tian and Y.-T. Long, *Sci. Rep.*, 2013, **3**, 1662.
18 F.-N. Meng, X. Yao, Y.-L. Ying, J. Zhang, H. Tian and Y.-T. Long, *Chem. Commun.*, 2015, **51**, 1202–1205.
19 Q. Jin, A. M. Fleming, Y. Ding, C. J. Burrows and H. S. White, *Biochemistry*, 2013, **52**, 7870–7877.
20 Q. Jin, A. M. Fleming, C. J. Burrows and H. S. White, *J. Am. Chem. Soc.*, 2012, **134**, 11006–11011.
21 X. Liang, H. Asanuma, H. Kashida, A. Takasu, T. Sakamoto, G. Kawai and M. Komiyama, *J. Am. Chem. Soc.*, 2003, **125**, 16408–16415.
22 D. W. Deamer and D. Branton, *Acc. Chem. Res.*, 2002, **35**, 817–825.
23 R. P. Johnson, R. T. Perera, A. M. Fleming, C. J. Burrows and H. S. White, *Faraday Discuss.*, 2016, **193**, 471–485.
24 C. Cao, Y.-L. Ying, Z.-L. Hu, D.-F. Liao, H. Tian and Y.-T. Long, *Nat. Nanotechnol.*, 2016, **11**, 713–718.
25 T. Goldau, K. Murayama, C. Brieke, S. Steinwand, P. Mondal, M. Biswas, I. Burghardt, J. Wachtveitl, H. Asanuma and A. Heckel, *Chem. - A Eur. J.*, 2015, **21**, 2845–2854.